Suppression of Beam Hosing in Plasma Accelerators with Ion Motion

T. J. Mehrling,* C. Benedetti, C. B. Schroeder, E. Esarey, and W. P. Leemans
Lawrence Berkeley National Laboratory, Berkeley, California 94720, USA

(Received 8 September 2018; revised manuscript received 19 November 2018; published 28 December 2018)

Mitigation of the beam hose instability in plasma-based accelerators is required for the realization of many applications, including plasma-based colliders. The hose instability is analyzed in the blowout regime including plasma ion motion, and ion motion is shown to suppress the hose instability by inducing a head-to-tail variation in the focusing force experienced by the beam. Hence, stable acceleration in plasma-based accelerators is possible, while, by use of proper bunch shaping, minimizing the energy spread and preserving the transverse beam emittance.

DOI: 10.1103/PhysRevLett.121.264802

Plasma based accelerators [1] are able to generate ultrahigh accelerating gradients, offering the possibility to deliver high energy charged particle beams over distances orders of magnitude smaller than achievable with conventional accelerator technology. This has attracted considerable interest in developing a plasma-based collider [2–5]. Transverse beam stability, i.e., suppressing beam hosing [6], has been identified as a critical challenge toward realizing a plasma-based collider. In beam hosing, the excited transverse wakefield of a beam couples to the beam transverse position, leading to exponential growth in the beam centroid displacement. This implies that small asymmetries or misalignments are exponentially amplified during the acceleration process. Variation of the transverse or longitudinal wakefields along the beam (head-to-tail) can mitigate hosing [7–9]. This mechanism is similar to the Balakin-Novokhatsky-Smirnov (BNS) damping of the beam-breakup instability in conventional accelerators [10]. However, plasma accelerators operate in a strongly beam-loaded regime for high efficiency, ideally generating non-varying longitudinal and transverse wakefields along the beam for quality preservation. The stable and quality preserving acceleration of witness beams therefore poses a crucial challenge in this strongly beam-loaded regime [11].

The high beam densities associated with collider-relevant beam parameters (high energy, high charge, and low emittance) induce a space charge force which moves the background ions on the timescale of the beam duration [12]. Ion motion has been identified as a potential source of emittance growth in plasma-based accelerators [12–14]; however, it has been shown that this emittance growth may be mitigated via slice-by-slice matching the transverse beam phase space distribution to the nonlinear ion-motion-perturbed plasma wakefields [14]. Ion motion will be relevant in near-future experiments (e.g., Ref. [15]).

In this Letter we show that ion motion can allow for stable and quality-preserving acceleration of witness beams in plasma-based accelerators. As we describe in this work, ion motion results in a head-to-tail variation in the focusing force provided by the background ions. Such a longitudinal variation results in a BNS-type damping of the hosing instability. We demonstrate this by deriving a theoretical model for the coupled evolution of the beam centroid and rms width along the beam with ion motion. This model is successfully compared to three-dimensional (3D) particle-in-cell (PIC) simulations with the quasistatic code HiPACE [16] for a case with nonrelativistic ion motion. After confirming the validity of our model we demonstrate via PIC simulations that hosing is suppressed within a single betatron period for witness beams with collider-relevant beam parameters, which excite relativistic ion motion. In addition, the preservation of the beam emittance can be realized through a slice-by-slice matching of the transverse beam distribution to the nonlinear wakefields [14] while the small energy spread is preserved by use of a tailored beam current profile [17].

In the following we consider a monoenergetic witness electron beam in the ion cavity driven by an intense laser or electron beam, i.e., in the nonlinear bubble [18] or blowout [19] regime. The witness beam may experience a constant accelerating gradient along the beam by shaping the longitudinal beam distribution [17]. The beam slices with centroid $X_b = \langle x \rangle$ are assumed to be Gaussian with an rms width of $\sigma_x^2 = \langle (x - X_b)^2 \rangle$, where $\langle \cdot \rangle$ represents the slice-dependent average with respect to the transverse phase space distribution. The slice emittance is assumed constant on the betatron timescale. The coupled differential equations for the first and second order moments for each longitudinal bunch slice are

$$\frac{d^2 X_b}{dz^2} = -\frac{k_p}{\gamma}\frac{\langle W_x \rangle}{E_0}, \tag{1a}$$

$$\frac{d^2 \sigma_x}{dz^2} = \frac{\epsilon_x^2}{\gamma^2 \sigma_x^3} - \frac{k_p \langle (x - X_b) W_x \rangle}{E_0 \gamma \sigma_x}, \tag{1b}$$

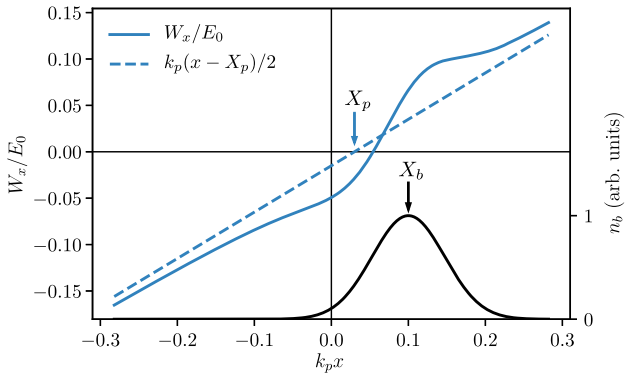

FIG. 1. Illustration of a wakefield W_x with hosing and nonrelativistic ion motion. The zero crossing of the homogeneous ion channel wakefield (dashed blue line) is shifted by the plasma electron centroid X_p due to hosing. In addition, ion motion causes a nonlinearity of the wakefield [solid blue line; see Eq. (2)]. Also depicted is a Gaussian distributed beam slice (black curve) with centroid X_b, subject to the force exerted by W_x.

where $W_x = E_x - B_y$ is the transverse wakefield acting on the beam electrons, $\epsilon_x = [\langle x^2\rangle\langle p_x^2\rangle - \langle x p_x\rangle^2]^{1/2}/mc$ is the phase-space emittance for each slice, γ the Lorentz factor of the monoenergetic beam, $k_p = \omega_p/c = (4\pi n_0 e^2/mc^2)^{1/2}$ the plasma wave number, and $E_0 = \omega_p mc/e$ the cold nonrelativistic wave breaking field, with e and m the electronic charge and mass, respectively, c the speed of light, and n_0 the ambient plasma electron density. For simplicity, the increase of beam energy is neglected here, which otherwise results in an adiabatic damping of X_b and σ_x. In the quasistatic approximation, and assuming nonrelativistic ion motion and beams short compared to the plasma ion wavelength, an expression for the transverse wakefield is given by [14]

$$\frac{W_x}{E_0} = \frac{k_p(x - X_p)}{2} - Z_i \frac{m}{M_i} k_p^2 \int_\infty^\zeta d\zeta'(\zeta - \zeta')\frac{E_{b,x}(\zeta')}{E_0}, \tag{2}$$

where $\zeta = z - ct$ is the longitudinal comoving coordinate, Z_i denotes the ionization level of the background ion species, M_i the ion mass, and $E_{b,x}$ the beam transverse electric field. Here X_p is the centroid of the plasma wake [20,21]. Figure 1 illustrates the relative centroids of a witness beam slice and the plasma wakefield. Ion motion causes a nonlinearity of the wakefield, which, in general, is shifted from the beam and plasma wake centroids.

We consider a cylindrically symmetric beam distribution with a small slice-dependent centroid perturbation $\delta X_b = X_b - X_{b0}$ with respect to the beam propagation axis $X_{b0} = X_b(\zeta = \zeta_0)$ (ζ_0 being the location of the bunch head),

$$n_b \simeq n_b^* - \delta X_b \cos(\theta)\frac{\partial n_b^*}{\partial r}, \tag{3}$$

where $n_b^*(\zeta, r) = \hat{I}_b g_\parallel(\zeta) g_\perp(\zeta, r)/ec$ is the cylindrically symmetric distribution with the peak beam current $\hat{I}_b$, an arbitrary longitudinal profile $g_\parallel(\zeta) \le 1$, and a slice-dependent Gaussian transverse profile $g_\perp(\zeta, r) = \exp[-r^2/2\sigma_x^2(\zeta)]/2\pi\sigma_x^2(\zeta)$, where $r = [(x - X_{b0})^2 + y^2]^{1/2}$ is the radius with respect to the beam propagation axis. The transverse electric field of the beam with a centroid perturbation is

$$E_{b,x} \simeq \cos(\theta) E_{b,r}^* - \delta X_b \left(\cos^2(\theta)\frac{\partial}{\partial r} + \frac{\sin^2(\theta)}{r}\right) E_{b,r}^*, \tag{4}$$

where $E_{r,b}^*$ is the radial field induced by the relativistic cylindrically symmetric Gaussian beam [14],

$$\frac{E_{b,r}^*(\zeta, r)}{E_0} = \frac{2\hat{I}_b}{I_A} g_\parallel(\zeta)\frac{\exp[-r^2/2\sigma_x^2(\zeta)] - 1}{k_p r}, \tag{5}$$

with the Alfvén current $I_A = mc^3/e \simeq 17$ kA. Combining Eqs. (2)–(5) yields

$$\frac{\langle W_x\rangle}{E_0} \simeq \frac{k_p[X_b(\zeta) - X_p(\zeta)]}{2} + Z_i \frac{m}{M_i}\frac{\hat{I}_b}{I_A} k_p \int_\infty^\zeta d\zeta'(\zeta - \zeta') g_\parallel(\zeta')\frac{X_b(\zeta) - X_b(\zeta')}{\sigma_x^2(\zeta) + \sigma_x^2(\zeta')} \tag{6}$$

and

$$\frac{k_p\langle(x - X_b)W_x\rangle}{E_0} \simeq \frac{k_p^2\sigma_x^2(\zeta)}{2} + Z_i \frac{m}{M_i}\frac{\hat{I}_b}{I_A} k_p^2 \int_\infty^\zeta d\zeta'(\zeta - \zeta') g_\parallel(\zeta')\frac{\sigma_x^2(\zeta)}{\sigma_x^2(\zeta) + \sigma_x^2(\zeta')}. \tag{7}$$

In Eqs. (6) and (7), terms $\mathcal{O}[\delta X_b^2(\zeta)] \ll \mathcal{O}(\sigma_x^2)$ and $\mathcal{O}[\delta X_b(\zeta)\delta X_b(\zeta')] \ll \mathcal{O}(\sigma_x^2)$ were neglected. Employing a model for the plasma wake centroid evolution along the beam, e.g., Refs. [20,21], Eqs. (1a) and (1b), with Eqs. (6) and (7), form a closed set of equations for $\sigma_x(\zeta, z)$, $X_b(\zeta, z)$, and $X_p(\zeta, z)$.

Note that for straight beams, Eq. (8) implies that $\langle W_x\rangle$ is identical to $k_p(X_b - X_p)/2$. However, if slices are misaligned with respect to the head of the beam, e.g., owing to hosing, various slices experience differing average wakefields. This head-to-tail variation in average wakefields can result in decoherence and suppression of the hosing (beam centroid) growth. Despite having the same effect of suppressing hosing through a head-to-tail decoherence, the above described mechanism is fundamentally different from the mechanism in the regime of linear plasma waves. In the linear regime, the decoherence is induced by a head-to-tail variation of the transverse wakefield and

the decoherence length depends only on the length and position of a monoenergetic beam in the plasma wave [9]. As seen from Eq. (6) and as illustrated in Fig. 1, ion motion has the effect of perturbing the wakefield, forcing beam slices to follow the head of the beam, and thereby inducing a head-to-tail variation of the average wakefield. The strength of this effect depends on the relative displacement, rms size, and current profile along the beam.

To gain further insight on the physics of the system, we consider the evaluation of Eqs. (1a), (1b), (6), and (7) with a simple two-particle (or two-slice, head-tail) model of the witness beam in the plasma wakefield: $g_{\parallel}(\zeta) = [\delta(\zeta-\zeta_0)+\delta(\zeta-\zeta_1)]L_b/2$, where $L_b = |\zeta_0-\zeta_1|$ is the length of the two-particle beam and ζ_0 and ζ_1 are the positions of the head and tail particles, respectively. The head particle oscillates according to $X_{b0}(z) = \hat{X}_{b,0}\cos(k_{\beta 0}z)$, where $\hat{X}_{b,0}$ is the initial offset of the particles and the betatron wave number of the head particle is $k_{\beta 0} = k_p/\sqrt{2\gamma}$. The transverse size of the beam head is matched to the homogeneous ion channel, such that $\sigma_{x0}^2 = \epsilon_x k_p^{-1}\sqrt{2/\gamma}$. The tail particle is assumed to be matched to the perturbed wakefield. The equilibrium solution of Eq. (1b) yields a matched rms size of $\sigma_{x1}^2 \simeq \sigma_{x0}^2(1-\Lambda/4)$ for $\Lambda \ll 1$, where $\Lambda = Z_i(m/M_i)(\hat{I}_b/I_A)(L_b^2/\sigma_{x0}^2)$ is a parameter that characterizes the amplitude of the ion motion perturbation. For $\sigma_{x1} = \text{const}$, the analytic solution of the centroid of the trailing particle using Eqs. (1a) and (6) is

$$\frac{X_{b1}}{\hat{X}_{b,0}} \simeq \cos(k_{\beta 1}z) + \alpha[\cos(k_{\beta 1}z) - \cos(k_{\beta 0}z)], \qquad (8)$$

where $k_{\beta 1}^2 \simeq k_{\beta 0}^2[1+\Lambda/2]$ and $\alpha = -2I_\zeta/\Lambda$, for $\Lambda \ll 1$. Here $I_\zeta = X_p(\zeta_1)/X_{b0}$ is a blowout-geometry-dependent constant, e.g., for the adiabatically generated blowout with nonrelativistic electron sheath, considered in Ref. [6], $I_\zeta = 1-\cos(k_p L_b/\sqrt{2})$. The difference of the betatron wave numbers in Eq. (8) is $\Delta k_\beta = k_{\beta 1}-k_{\beta 0} \simeq k_{\beta 0}\Lambda/4$, such that the decoherence length is $k_{\beta 0}L_d \simeq 4\pi/\Lambda$ for $\Lambda \ll 1$. For a hydrogen plasma with density $n_0 = 10^{17}$ cm^{-3}, $\Lambda \simeq 6.0\times 10^{-5}\hat{I}_b(\text{kA})[L_b(\mu\text{m})]^2[E(\text{GeV})]^{1/2}[\epsilon_x(\mu\text{m})]^{-1}$. For example, a beam with $\epsilon_x = 1.0$ μm, a current of $\hat{I}_b = 17$ kA, a length of $L_b = 20$ μm, and an energy of $E = 1$ GeV yields $\Lambda \simeq 0.36$, such that a full head-to-tail decoherence is reached after a distance of $k_{\beta 0}L_d = 34.9$, or, equivalently, after ~6 betatron periods.

We validated the proposed model by comparing its predictions with results from 3D PIC simulations performed with the quasistatic code HiPACE [16]. We consider a witness beam with the parameters above, causing nonrelativistic ion motion ($\Lambda \simeq 0.36$). The beam has a flat-top current profile with $\hat{I}_b/I_A = 1.0$, a length $k_p L_b = 1.2$, energy of $\gamma = 1000$, and emittance $k_p\epsilon_x = 0.07$ such that $\sigma_{x0} = (\epsilon_x/k_p)^{1/2}(2/\gamma)^{1/4} = 0.047k_p^{-1} = 0.79$ μm in the blowout wake with background density $n_0 = 10^{17}$ cm^{-3}. The blowout wake is generated by an electron drive beam with $n_b^{(d)}/n_0 = 4$, $\sigma_x^{(d)} = \sigma_y^{(d)} = 0.8k_p^{-1}$, and $\sigma_z^{(d)} = \sqrt{2}k_p^{-1}$ in a hydrogen plasma. The witness beam current profile starts at a distance of $5k_p^{-1}$ behind the center of the drive beam. To isolate the effect of the ion motion on hosing, and for an easier comparison with theory, the witness beam was initialized monoenergetic and its energy was kept constant in the PIC simulation in this case. Initially, the witness beam is misaligned by $\hat{X}_{b,0} = 0.1\sigma_{x0}$ from the drive beam propagation axis. In the PIC simulations, we use a box with dimensions $16\times 16\times 11.5k_p^{-3}$, and cell size $0.031\times 0.031\times 0.02k_p^{-3}$. In the witness beam region we employ a refined mesh with a resolution of $\Delta_x = \Delta_y = 1.1\times 10^{-3}k_p^{-1}$ and $\Delta_\zeta = 6.4\times 10^{-3}k_p^{-1}$. The witness beam consists of 10^7 numerical particles. The plasma electrons are rendered with 4 numerical particles per cell (p.p.c.) in the center and 1 p.p.c. close to the transverse computational box boundaries. The plasma ions are sampled with 9 p.p.c. in the center and no particles (assuming a static ion background) close to the transverse computational box boundaries. The quasistatic time step is $5\omega_p^{-1}$, and a tenfold subcycling is used to push the witness beam particles. PIC modeling results were compared with numerical solutions of Eqs. (1a) and (1b), with Eqs. (6) and (7), where the model presented in Ref. [21] was used to describe the plasma wake centroid X_p. Figure 2 shows the displacement of the witness beam tail centroid versus propagation distance $k_{\beta 0}z$, with and without ion motion as predicted by the model and obtained with PIC simulations. We see that ion motion suppresses the growth of the centroid displacement. The suppression occurs over a decoherence length, approximately ~6 betatron periods, as predicted by the simple two-particle model.

For collider-relevant witness beam parameters (i.e., high energy, high charge, and low emittance), the motion of the ions may be relativistic, i.e., $\Lambda \gg 1$. In this regime ion

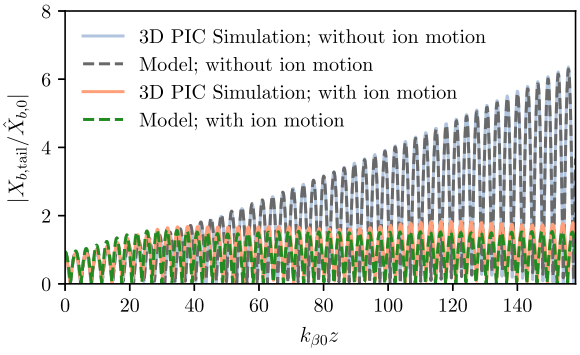

FIG. 2. Beam tail centroid displacement predicted by the model presented in this Letter (dashed lines) and by 3D PIC simulations (solid lines), with and without ion motion. Ion motion suppresses hosing and the suppression occurs over the decoherence length $k_{\beta 0}L_d = 34.9$, approximately after ~6 betatron periods for the parameters considered, as predicted by the two-particle model.

motion in a plasma-based accelerator will also suppress the hosing. To demonstrate this, we consider a PIC simulation of a beam with an initial energy of 25 GeV ($\gamma_0 = 49000$) and an emittance $\epsilon_x = 0.26\ \mu$m, in a blowout wake (the background plasma is hydrogen with $n_0 = 10^{17}\ \mathrm{cm}^{-3}$) such that the linearly matched rms size, i.e., the matched beam size assuming a homogeneous ion channel, is $\sigma_{x0} = (\epsilon_x/k_p)^{1/2}(2/\gamma_0)^{1/4} = 0.01 k_p^{-1} = 0.17\,\mu$m. The beam has a length of $L_b = 2.0 k_p^{-1} = 33.6\ \mu$m, and a trapezoidal current profile ranging from 27 kA at the head to 17 kA at the tail such that the blowout wake is optimally loaded, generating a constant longitudinal electric field along the beam, so that the energy spread (initially zero) remains small ($< 0.1\%$) during acceleration. The blowout wake is generated by a particle drive beam with $n_b^{(d)}/n_0 = 4$, $\sigma_x^{(d)} = \sigma_y^{(d)} = 0.8 k_p^{-1}$, and $\sigma_z^{(d)} = \sqrt{2} k_p^{-1}$ in a hydrogen plasma. The witness beam current profile starts at a distance of $5 k_p^{-1}$ behind the center of the drive beam. Initially, the witness beam is misaligned by $\hat{X}_{b,0} = \sigma_{x0}$ from the drive beam propagation axis. For the above parameters $\Lambda \sim 35$, so that in this regime we expect ion motion to suppress the beam centroid growth within a single betatron period.

In the PIC simulations, we use a box with dimensions $16 \times 16 \times 11.5 k_p^{-3}$, and cell size $0.031 \times 0.031 \times 0.02 k_p^{-3}$. In the witness beam region we employ a refined mesh with resolution $\Delta_x = \Delta_y = 5.9 \times 10^{-4} k_p^{-1}$ and $\Delta_\zeta = 6.4 \times 10^{-3} k_p^{-1}$. The witness beam consists of 10^7 numerical particles. The plasma electrons are sampled with 4 p.p.c. in the center and 1 p.p.c. close to the transverse computational box boundaries. The plasma ions are sampled with 9 p.p.c. in the center and no particles (assuming a static ion background) close to the transverse box boundaries. The quasistatic time step is $\geq 15\omega_p^{-1}$, where a dynamic time-step adjustment and a tenfold subcycling to push the witness beam particles is used.

Figure 3 (top) shows the growth the centroid displacement observed in the PIC simulation at the tail of the witness beam versus propagation distance $k_{\beta,0} z$, where $k_{\beta,0} = k_p (2\gamma_0)^{-1/2}$ is the initial betatron wave number. Shown are the results from a simulation neglecting ion motion (gray dashed curve) and from two simulations with ion motion for different transverse beam distributions (red dashed curve and green curve). It can be observed that hosing is suppressed in the cases with ion motion while, neglecting ion motion, hosing results in an amplification of the beam centroid.

As shown in Fig. 3 (bottom), hosing leads to a continual growth of the projected transverse emittance owing to the increasingly misaligned slices along the beam for the case where ion motion is neglected (gray dashed curve). A beam which is conventionally (linearly) matched, i.e., assuming a homogeneous ion channel and injecting at the respective beta function of $k_\beta^{-1} = k_p^{-1}(2\gamma)^{1/2}$ (the rms size is thereby constant along the beam), also undergoes an emittance

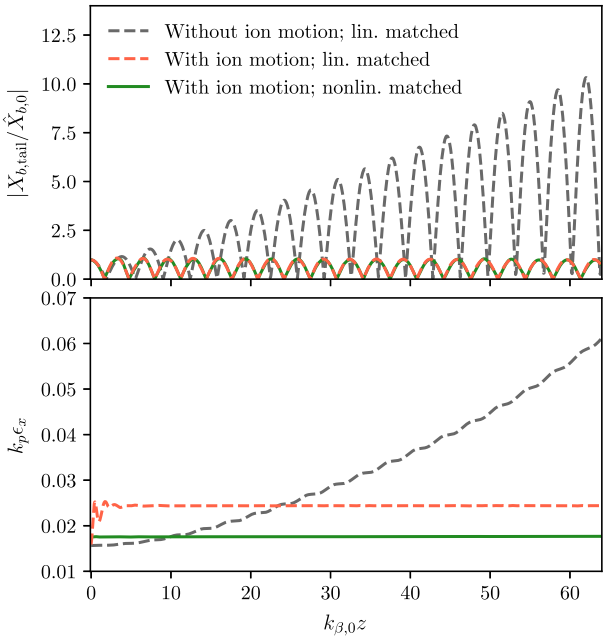

FIG. 3. Top: Comparison of the centroid amplitude at the tail of a witness beam, computed using 3D PIC simulations, for a linearly matched beam (red dashed) and a nonlinearly matched beam (green solid). As a comparison, a simulation result neglecting ion motion effects is shown (gray dashed). Bottom: Respective evolution of the projected beam emittance for the three cases.

deterioration as shown by the red dashed curve in Fig. 3 (bottom). Since hosing is suppressed and since the ion motion is symmetric with respect to the symmetry axis of the beam, the mechanism of emittance growth is solely due to the ion-motion-induced nonlinearity of the transverse wakefields, discussed in Refs. [12–14]. The beam emittance grows over the first few betatron periods owing to a betatron phase decoherence and saturates as soon as the beam distribution is matched to the nonlinear fields owing to complete phase mixing (red dashed curve for $k_{\beta,0} z \gtrsim 5$). However, emittance growth can be completely eliminated by using a witness beam with a transverse phase-space distribution that is, slice-by-slice, nonlinearly matched to the ion-motion-perturbed transverse wakefields (green curve). The transverse phase space distribution of such nonlinearly matched beams is slice by slice an equilibrium solution of the Vlasov equation for the respective ion-motion-perturbed wakefield, as described in detail in Ref. [14]. Such slice-by-slice matched distributions can be generated adiabatically from linearly matched distributions during the acceleration in the plasma without significant emittance deterioration [22]. Hence, ion motion suppresses the hose instability, and a proper slice-by-slice transverse matching also ensures the emittance preservation in the ion-motion perturbed wakefields.

In this Letter, we have demonstrated that the ion motion induced by a witness electron beam in the nonlinear

blowout wake of an intense driver (laser or particle beam) will suppress the hosing instability owing to the ion-motion-induced head-to-tail variation in the focusing force. A model was developed to describe the beam motion (beam centroid and spot size evolution) in the plasma wakefield including the influence of ion motion. This model was compared to PIC simulations in the regime of validity, and good agreement was found. Suppression of the hosing instability occurred over a decoherence length. For collider-relevant beam parameters (high energy, high charge, and low emittance) the ion motion is relativistic and hosing suppression occurs within one betatron period. By using a witness beam with a transverse phase-space distribution that is slice-by-slice matched to the ion-motion-perturbed wakefield, emittance growth from both hosing and ion motion may be eliminated. If the bunch current distribution is also shaped to beam load the longitudinal wake such that a constant accelerating gradient is achieved, energy spread growth will also be minimized. Hence, by proper beam shaping, ion motion may be employed to provide stable and quality-preserving plasma-based acceleration of electron beams.

This work was supported by the Director, Office of Science, Office of High Energy Physics, of the U.S. Department of Energy under Contract No. DE-AC02-05CH11231 and used the computational facilities at the National Energy Research Scientific Computing Center (NERSC).

*tjmehrling@lbl.gov

[1] E. Esarey, C. B. Schroeder, and W. P. Leemans, Rev. Mod. Phys. **81**, 1229 (2009).
[2] W. Leemans and E. Esarey, Phys. Today **62**, No. 3, 44 (2009).
[3] C. B. Schroeder, E. Esarey, C. G. R. Geddes, C. Benedetti, and W. P. Leemans, Phys. Rev. ST Accel. Beams **13**, 101301 (2010).
[4] A. Seryi, M. Hogan, S. Pei, T. Raubenheimer, P. Tenenbaum, T. Katsouleas, C. Huang, C. Joshi, W. Mori, and P. Muggli, in *Proceedings of the 23rd Conference, PAC'09, Vancouver, Canada, 2009* (2010), WE6PFP081.
[5] E. Adli, J.-P. Delahaye, S. J. Gessner, M. J. Hogan, T. Raubenheimer, W. An, C. Joshi, and W. Mori, in *Proceedings, 2013 Community Summer Study on the Future of U.S. Particle Physics: Snowmass on the Mississippi (CSS2013): Minneapolis, 2013* (2013) [arXiv:1308.1145].
[6] D. H. Whittum, W. M. Sharp, S. S. Yu, M. Lampe, and G. Joyce, Phys. Rev. Lett. **67**, 991 (1991).
[7] J. Vieira, W. B. Mori, and P. Muggli, Phys. Rev. Lett. **112**, 205001 (2014).
[8] T. J. Mehrling, R. A. Fonseca, A. Martinez de la Ossa, and J. Vieira, Phys. Rev. Lett. **118**, 174801 (2017).
[9] R. Lehe, C. B. Schroeder, J.-L. Vay, E. Esarey, and W. P. Leemans, Phys. Rev. Lett. **119**, 244801 (2017).
[10] V. E. Balakin, A. V. Novokhatsky, and V. P. Smirnov, in *Proceedings, 12th International Conference on High-Energy Accelerators, HEACC 1983: Fermilab, Batavia* (1984), pp. 119–120.
[11] V. Lebedev, A. Burov, and S. Nagaitsev, Phys. Rev. Accel. Beams **20**, 121301 (2017).
[12] J. B. Rosenzweig, A. M. Cook, A. Scott, M. C. Thompson, and R. B. Yoder, Phys. Rev. Lett. **95**, 195002 (2005).
[13] W. An, W. Lu, C. Huang, X. Xu, M. J. Hogan, C. Joshi, and W. B. Mori, Phys. Rev. Lett. **118**, 244801 (2017).
[14] C. Benedetti, C. B. Schroeder, E. Esarey, and W. P. Leemans, Phys. Rev. Accel. Beams **20**, 111301 (2017).
[15] M. Hogan, Report No. SLAC-R-1072, Technical Design Report for the FACET-II Project at SLAC National Accelerator Laboratory, SLAC Report, 2017.
[16] T. Mehrling, C. Benedetti, C. B. Schroeder, and J. Osterhoff, Plasma Phys. Controlled Fusion **56**, 084012 (2014).
[17] M. Tzoufras, W. Lu, F. S. Tsung, C. Huang, W. B. Mori, T. Katsouleas, J. Vieira, R. A. Fonseca, and L. O. Silva, Phys. Rev. Lett. **101**, 145002 (2008).
[18] A. Pukhov and J. Meyer-ter Vehn, Appl. Phys. B **74**, 355 (2002).
[19] J. B. Rosenzweig, B. Breizman, T. Katsouleas, and J. J. Su, Phys. Rev. A **44**, R6189 (1991).
[20] C. Huang, W. Lu, M. Zhou, C. E. Clayton, C. Joshi, W. B. Mori, P. Muggli, S. Deng, E. Oz, T. Katsouleas, M. J. Hogan, I. Blumenfeld, F. J. Decker, R. Ischebeck, R. H. Iverson, N. A. Kirby, and D. Walz, Phys. Rev. Lett. **99**, 255001 (2007).
[21] T. J. Mehrling, C. Benedetti, C. B. Schroeder, A. Martinez de la Ossa, J. Osterhoff, E. Esarey, and W. P. Leemans, Phys. Plasmas **25**, 056703 (2018).
[22] T. J. Mehrling *et al.* (to be published).